

Improved earthquake-resistant design methods of shallow coupling beams

Myoungsu Shin^{1)*}, Seong Woo Gwon²⁾, Kihak Lee³⁾ and Sang Whan Han⁴⁾

^{1), 2)} School of Urban and Environmental Engineering, UNIST, Ulsan, Korea

³⁾ Department of Architectural Engineering, Sejong University, Seoul, Korea

⁴⁾ Department of Architectural Engineering, Hanyang University, Seoul, Korea

¹⁾ msshin@unist.ac.kr

ABSTRACT

Presented is an experimental study aimed at improving the earthquake-resistant design of reinforced concrete shallow coupling beams in a coupled shear wall system. In particular, the use of high performance fiber-reinforced cement composites (HPFRCC) is explored as an innovative method of improving the seismic capacity of shallow coupling beams and reducing transverse reinforcement requirements for such beams. Six 1/2-scale coupling beams having the length-to-depth ratio of 3.5 were tested under cyclic lateral loading up to 10% drift. The key test variables were main reinforcement layout, material type, and transverse reinforcement ratio. Two types of main reinforcement layout were tested: conventional and diagonal reinforcement. For the material type, normal concrete and HPFRCC using PVA fibers of 2% volumetric ratio were compared. The amount of transverse reinforcement varied to be about 0, 50, and 100% of the minimum specified in Chapter 21 of ACI 318-11.

1. INTRODUCTION

Reinforced concrete (RC) coupling beams in coupled wall systems designed based on current codes are expected to endure significant inelastic deformations, when subjected to design-level earthquakes. Suitably devised coupling beams may be able to serve as primary sources for energy dissipation (Paulay 1992).

In high-rise residential buildings of which the seismic force-resisting system consists of shear walls combined with RC slab-column frames, the depth of coupling beams is typically limited due to relatively small story heights. Although this type of construction has been popularly used for many decades, the seismic design of shallow coupling beams has not been investigated much, which is the main subject of this study. Most of the previous studies focused on deep coupling beams, and examined various reinforcement details to propose proper methods of ensuring satisfactory ductility and relieving steel congestion (Fortney 2008).

High performance fiber-reinforced cement composites (HPFRCCs) are

¹⁾ Assistant Professor, Corresponding Author

²⁾ Graduate Student

³⁾ Professor

⁴⁾ Professor

characterized by strain-hardening response in direct tension by developing multiple micro-cracks with assistance of engineered fibers (Naaman 2003, Kim 2009). HPFRCCs generally show high ductility under both tension and compression, so that confinement requirements may be relaxed in members of high reinforcement congestion by using HPFRCCs (Parra-Montesinos 2005). When subjected to seismic forces, HPFRCCs are deemed to also improve energy dissipation through fiber bridging over micro-cracks and by providing excellent bond between reinforcing steel and cement composites (Li 2003). During the last decade, several leading research groups played major roles in large-scale experimental investigations for the effectiveness of HPFRCCs in earthquake-resistant structures. Most of them tested shear-dominated members such as deep coupling beams, beam-column joints, slab-column connections, and infill panels (Parra-Montesinos 2005).

However, only a few tests involved flexure-dominated members. Given the concerns, this study explores the use of HPFRCC as an innovative method of improving the seismic capacity of shallow coupling beams and reducing transverse reinforcement requirements for such beams.

2. DESCRIPTION FOR EXPERIMENTAL TESTS

Six approximately 1/2-scale coupling beam specimens were tested under lateral cyclic loading (Figure 1). Each specimen represented a shallow coupling beam that is part of a coupled shear wall system combined with flat plates in a tall residential building. The testing program proceeded in two series: Series-1 (1DF0Y, 1DF2Y, and 1CF2Y) and Series-2 (2DF0Y, 2DF2H, and 2DF2N).

2.1 Specimen Details and Test Variables

Figure 1 illustrates elevation views of the specimens. In all specimens, the beam width (b) was 250 mm, the beam depth (h) was 300 mm, and the length (l) of the beam was 1050 mm, so that the length-to-depth ratio (l/h) was 3.5. Table 1 summarizes the design details and test variables of the six specimens. The key test variables were (1) main reinforcement layout, (2) material type, and (3) transverse reinforcement ratio. Two types of main reinforcement layout were tested: conventional and diagonal layouts. Specimen 1CF2Y was reinforced with the conventional layout, while the other five specimens were with the diagonal layout. The amount of longitudinal reinforcement (Table 1) was determined so that the maximum shear stress level (V_{max}/bh) in the beam is approximately equal to $0.5\sqrt{f'_c}$ (MPa) in all specimens, where V_{max} is the maximum beam shear assumed to be governed by the yielding of longitudinal bars.

In the diagonal layout, transverse reinforcement were provided for the entire section of the beam as an alternative to enclosing each group of diagonal bars, and horizontal bars used to anchor transverse ties had a short embedded length into the stubs in order not to develop yielding. For the material type, one type of HPFRCC using PVA fibers of 2% volumetric ratio was compared with normal concrete. Four of the specimens were constructed with the HPFRCC, while two (1DF0Y, 2DF0Y) with normal

concrete. The amount of transverse reinforcement varied to be about 0, 50, and 100% of the minimum required by ACI 318-11, §21.9.7.4.

Table 1 Design details and test variables

Specimen	Aspect Ratio	Reinf. Layout	Material type	Longi. reinf.	Trans. reinf.	f'_c (MPa) Concrete or HPFRCC
1CF2Y	3.5	Conventional	HPFRCC (PVA 2%)	3 D25 @ top & bot.	D10 @ 65 mm	49.2
1DF0Y		Diagonal	Concrete	4 D25 @ each diag.	D13 @ 120 mm	29.2
1DF2Y			HPFRCC (PVA 2%)	4 D25 @ each diag.	D13 @ 120 mm	49.2
2DF0Y			Concrete	4 D25 @ each diag.	D13 @ 110 mm	44.1
2DF2N			HPFRCC (PVA 2%)	4 D25 @ each diag.	-	40.1
2DF2H			HPFRCC (PVA 2%)	4 D25 @ each diag.	D13 @ 220 mm	40.1

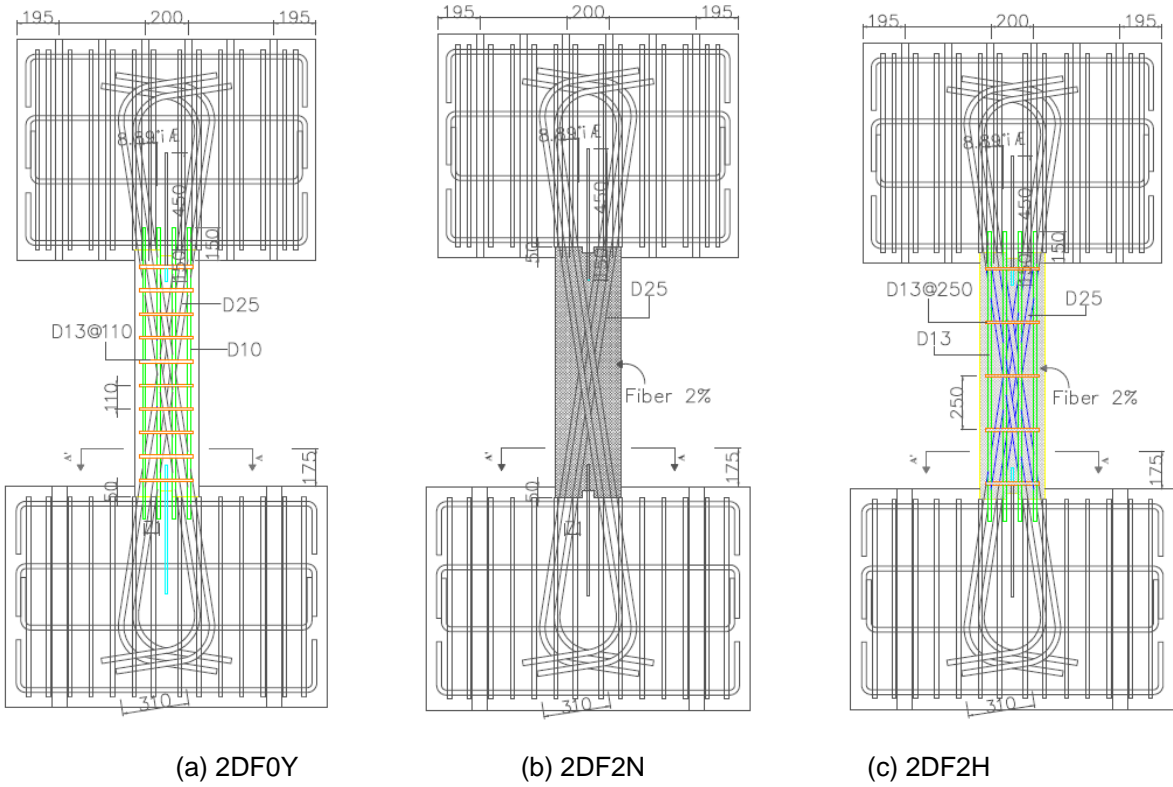


Fig. 1 Elevation views of the specimens (Series-2)

In each specimen, the coupling beam portion had been cast first, and the top and bottom stubs that simulated the behavior of coupled shear walls were cast about a week later. The ends of the beam were connected to the stubs with the help of tooth-shaped concrete shear keys and dowel bars, as well as the dowel action of longitudinal bars. For the four HPFRCC specimens, the HPFRCC was used only for the beam portion, while the stubs were made with normal concrete. Table 1 summarizes the compressive strength (f'_c) of the HPFRCC or normal concrete measured on the testing day. Physical properties of the PVA fibers used are summarized in Table 2.

Table 2 Physical properties of PVA fibers

Fiber type	Density (g/m ³)	Tensile strength (MPa)	Elastic modulus (GPa)	Diameter (μ m)	Length (mm)	Volume in HPFRCC
PVA	1.3	1600	25	39	12	2%

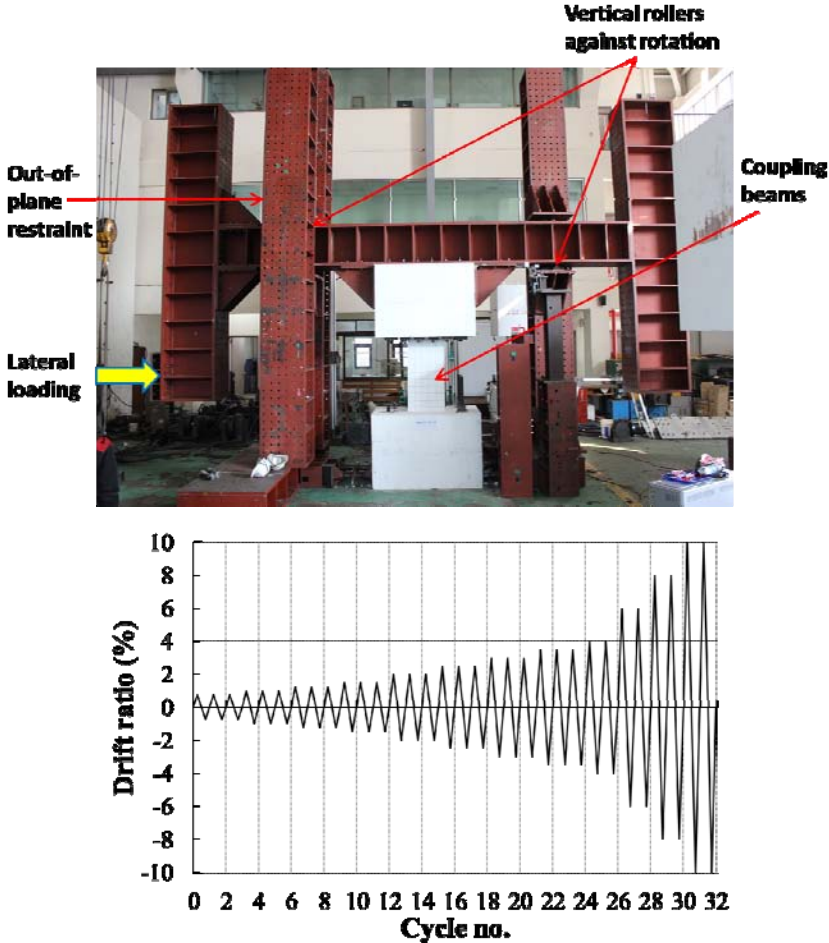


Fig. 2 Test setup and loading history (Series-1)

2.2 Test Setup and Loading History

Figure 2 illustrates the test setup and loading history used for the Series-1 tests. The specimen was tested in a configuration that the coupling beam was vertically oriented. The bottom RC stub was anchored to the strong floor, and the top RC stub was linked to the horizontal segment of the loading frame by anchor rods. Reversed cyclic loading was statically applied by an actuator to the vertical segment of the loading frame, which was rigidly connected to the horizontal segment. The longitudinal axis of the actuator was arranged to pass through the midspan of the coupling beam, in order to simulate zero moment at the midspan. Two vertical pin-ended supports were used; the bottom of each support was anchored to the strong floor, and the top was to the horizontal segment of the loading frame. The vertical supports were to prevent the top of the coupling beam from rotating about an out-of-plane axis and to restrain axial elongation of the beam.

Reversed displacement cycles in Figure 2 were statically applied up to 10% drift ratio. Two or three consecutive same-drift cycles were tested to examine strength and stiffness degradations under repeated loading.

3. DISCUSSION OF TEST RESULTS

Extensive investigations are underway on the test results including the cracking and failure mode, load-displacement response (i.e., strength, stiffness, ductility, energy dissipation), and various deformations (e.g., flexural rotations, shear distortions) of each specimen. In this paper, only preliminary findings and conclusions are discussed.

3.1 Failure Mode

Figure 3 illustrates cracking patterns observed in the six specimens: at the end of testing (i.e., 5% drift) in 2DF2N and at 10% drift in the other specimens. Specimen 1DF2Y experienced no apparent failure, which showed the least damage among the tested specimens. The specimens of normal concrete (1DF0Y and 2DF0Y) suffered much more severe cracking damage; a relatively small number of inclined cracks widely opened in the normal concrete specimens, while numerous thin cracks occurred in the HPFRCC specimens. The two normal concrete specimens that were designed following ACI 318-11 (2011) underwent flexural failure in the end.

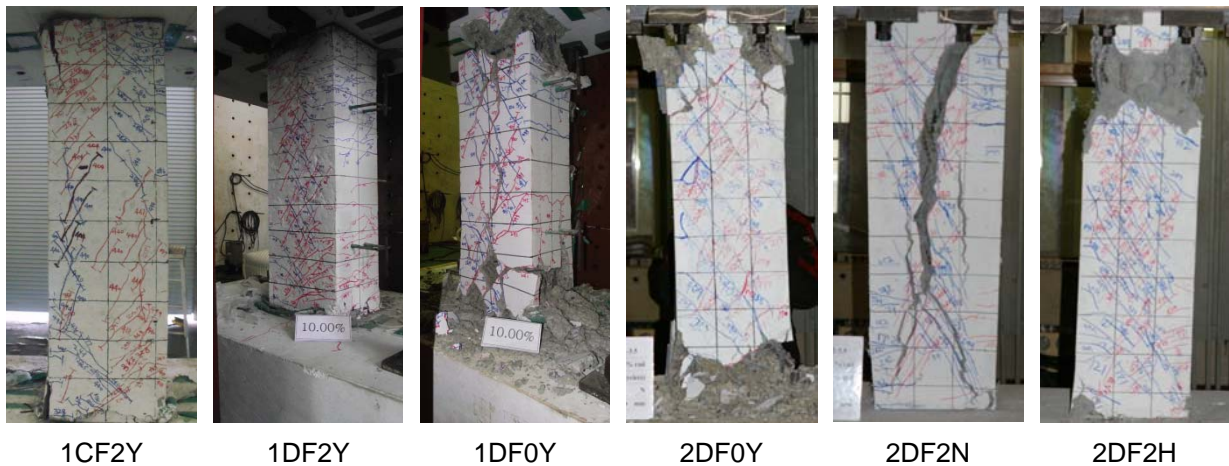


Fig. 3 Cracking damage at 10% drift (exception: 5% drift for 2DF2N)

Specimen 1CF2Y with the conventional reinforcement layout displayed relatively minor cracking damage. However, 1CF2Y eventually underwent flexural failure followed by the yielding of transverse steel. At each end of the beam, the HPFRCC in compression was crushed during the 3.5% drift cycles. Then, higher stresses appeared to concentrate in the longitudinal bars (partially due to residual strains in the bars), so that the bars were forced to buckle out, and consequently stressed adjacent transverse reinforcement.

Specimen 2DF2H having 50% reduced transverse steel achieved a well-developed flexural mechanism up to the 7% drift cycles. During the second cycle to negative 7% drift, however, 2DF2H experienced the buckling of the diagonal bars near the top end of the beam (Figure 3), due to the wider spacing of transverse reinforcement. Specimen 2DF2N with no transverse reinforcement collapsed much earlier than the other specimens, showing several large inclined (diagonal tension) cracks crossing over the entire span. Nevertheless, 2DF2N was able to sustain the wide growth of the inclined cracks up to 5% drift.

3.2 Overall Load-Displacement Response

Figure 4 shows the cyclic lateral load-drift responses of the six specimens. The drift is defined as the lateral displacement applied at the top of the coupling beam divided by the beam length (δ).

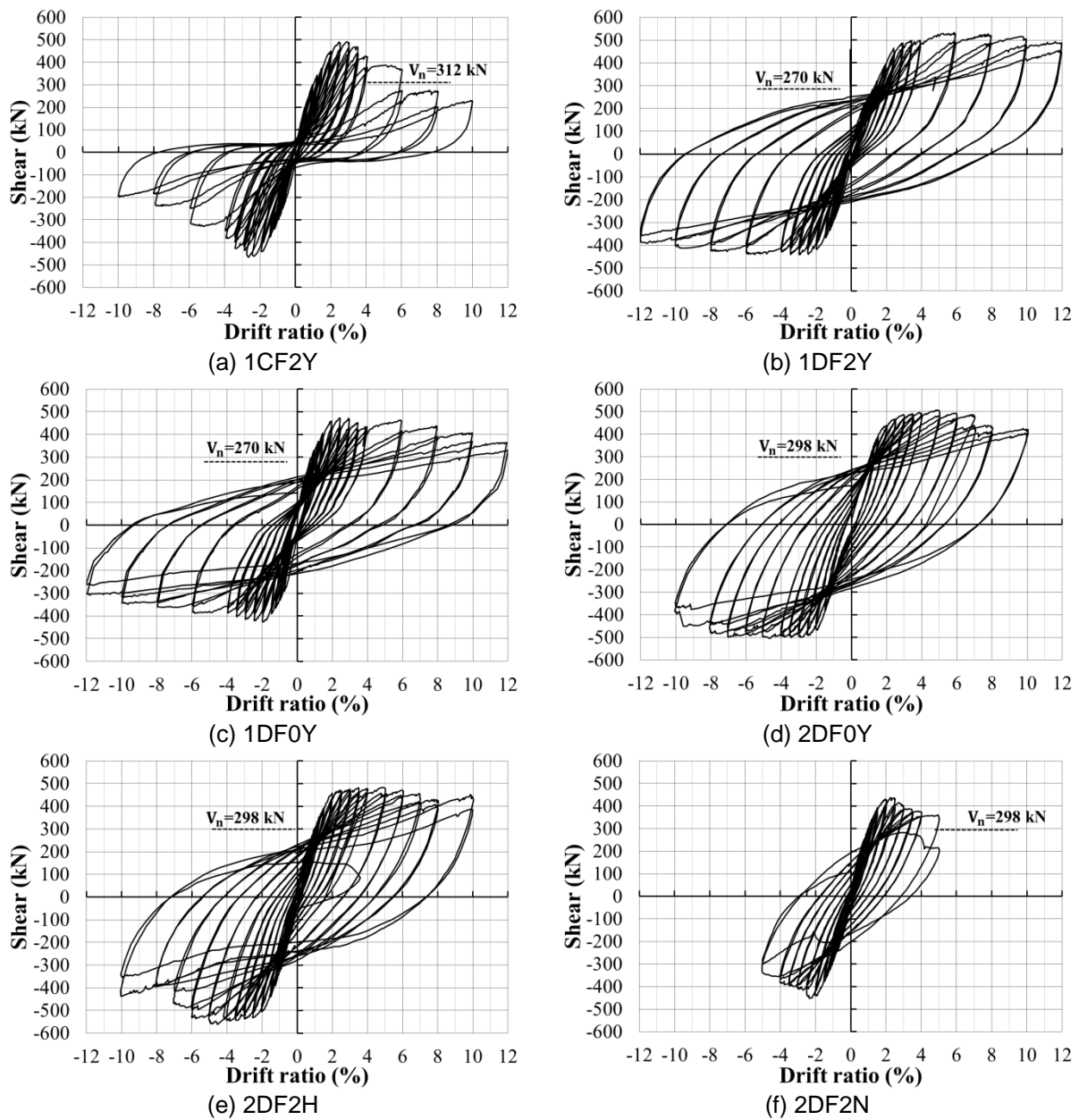


Fig. 4 Lateral load-drift responses

Of the Series-1 specimens, 1DF2Y exhibited the most stable load-displacement behavior; the lateral load barely reduced by the end of testing, and almost no pinching was detected in the hysteretic loops. Similarly, Specimen 1DF0Y developed a stable load-drift response by the end of testing, but showed gradual strength degradation after the 6% drift cycles. In contrast, 1CF2Y underwent relatively fast strength degradation after the 3% drift cycles, attaining the smallest displacement ductility, and it showed severe pinching in the cyclic load-drift responses. This implies that the diagonal layout of main longitudinal bars was much more functional than the conventional layout in the

shallow coupling beams.

Among the Series-2 tests, 2DF2H exhibited a satisfactory load-drift response that was comparable to that of 2DF0Y, the normal concrete specimen having transverse steel conforming to ACI 318-11 (2011). (On the other hand, 2DF2H showed relatively large strength drops at the 7 and 8% drift cycles in the negative loading, likely due to the buckling of the diagonal bars.) Also, Specimen 2DF2N with no transverse steel achieved a moderate level of displacement ductility equal to approximately 3.5, although it eventually underwent shear (diagonal tension) failure as a couple of inclined cracks widely opened (see Figure 3). This indicates that the HPFRCC supplied significant confinement to the diagonal bars, which typically tend to buckle in the inelastic range, when the ends of the coupling beam are subjected to moment reversals.

3.3 Energy Dissipation

The amount of energy dissipated during a loading cycle is taken as the area enclosed by the corresponding load-displacement hysteretic curve. Figures 5(a) and 5(b) illustrate the energy dissipated during the first cycle to each drift ratio in the Series-1 and Series-2 specimens, respectively.

In Series-1, the two specimens having diagonal reinforcement (1DF0Y and 1DF2Y) presented comparable energy dissipations throughout the tests; the effect of the HPFRCC was not eminent in the diagonally reinforced coupling beams. In contrast, the dissipated energy of 1CF2Y having conventional reinforcement got apparently smaller than those of the other specimens from about 6% drift, at which 1CF2Y underwent sudden strength degradation. At the end of the 10% drift cycles, the cumulated energy in 1CF2Y was less than 50% of those in the other specimens. Therefore, it may be said that the use of diagonal reinforcement greatly improved the energy-dissipating capability of the shallow coupling beams.

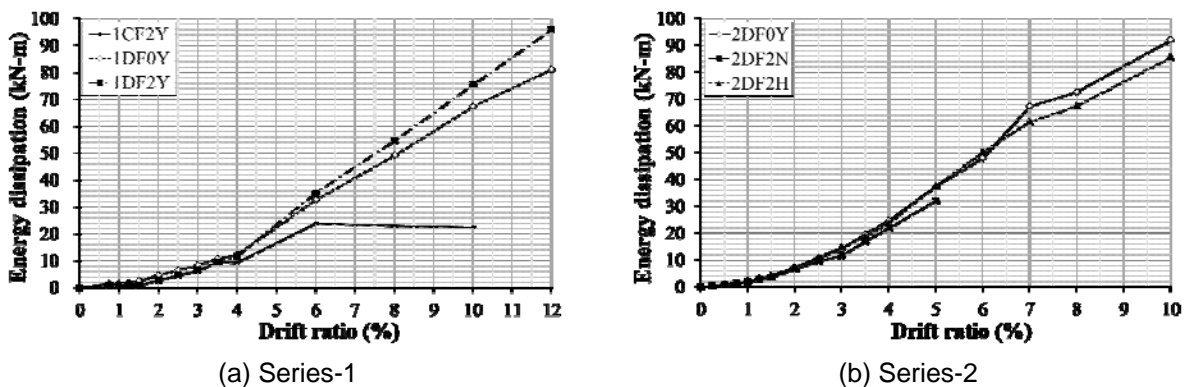


Fig. 5 Energy dissipated per 1st cycle to each drift

In the Series-2 tests, 2DF2H having 50%-reduced transverse steel achieved very similar energy dissipation to 2DF2Y by the end of testing. Also, 2DF2N having no transverse steel showed only slightly smaller amounts of energy dissipation until it collapsed at 5% drift. This is supportive evidence that the use of the HPFRCC improved the energy dissipation capacity of the shallow coupling beams, likely through fiber-bridging action across multiple micro-cracks (Li 2003).

3.4 Strength Prediction

Specimen 1DF2Y achieved the greatest maximum load, 12% higher than that of 1DF0Y in the positive loading; this was likely attributed to the effect of the HPFRCC on the flexural strength of the beam. In contrast, Specimen 2DF2N showed the smallest maximum load, lower than those of 2DF2Y and 2DF2H; the strength of 2DF2N deemed limited by diagonal tension failure.

The strength of each specimen (V_n) is predicted as the lateral load corresponding to the nominal moment strength (M_n) of the coupling beam (i.e., $V_n = 2M_n/l$), determined based on ACI 318-11 (2011): Section 10.2 for 1CF2Y with conventional reinforcement, and Section 21.9.7 for the other specimens with diagonal reinforcement. Note that M_n is estimated ignoring effects of the HPFRCC on the compressive and tensile stress-strain relationships, as well as effects of the axial load that would be imposed in the coupling beam.

As shown in Figure 4, the measured maximum load was much larger than the predicted strength in all specimens. This is true even in Specimen 2DF2N of which the maximum load deemed to be limited by diagonal tension failure. The higher measured strength seems to have resulted primarily from the axial load (compression) naturally imposed in the coupling beam by the loading frame system; elongation of the coupling beam due to concrete cracking and inelastic residual strains in the longitudinal bars was restrained, as in a real structure. The results imply that the coupling beams designed based on the current codes would actually achieve much higher strengths than those expected by the codes. To more accurately predict the strength of each specimen, the axial loads imposed in the coupling beam are estimated using the data measured by the load cells at the vertical supports.

4. CONCLUSIONS

The diagonal reinforcement layout, compared with the conventional layout, greatly improved the energy dissipation and ductility of the shallow coupling beams. The confining effect of the HPFRCC enabled to reduce at least 50% of the transverse steel required by ACI 318-11 for diagonally reinforced coupling beams. The measured maximum load was much larger than the predicted strength in all specimens, which seems to have resulted primarily from the axial load naturally imposed in the coupling beam.

ACKNOWLEDGEMENTS

This research was supported by Basic Science Research Program through the National Research Foundation of Korea (NRF) funded by the Ministry of Education, Science and Technology (Grant No. 2010-0022955).

REFERENCES

- ACI Committee 318 (2008), *Building Code Requirements for Reinforced Concrete (ACI 318-08) and Commentary (ACI 318R-08)*, American Concrete Institute, Farmington Hills, Michigan, 503 pp.
- Fortney, P.J., Rassati, G.A. and Shahrooz, B.M. (2008), "Investigation on effect of transverse reinforcement on performance of diagonally reinforced coupling beams", *ACI Structural Journal*, Vol. **105**(6), 781-788.
- Kim, D.J., Naaman, A.E. and El-Tawil, S. (2009), "High performance fiber reinforced cement composites with innovative slip hardening twisted steel fibers", *International Journal of Concrete Structures and Materials*, Vol. **3**(2), 119-126.
- Li, V. (2003), "On Engineered Cementitious Composites (ECC); a review of the material and its application", *Journal of Advanced Concrete Technology*, Vol. **1**(3), 215-230.
- Naaman, A.E. (2003), "Engineered steel fibers with optimal properties for reinforcement of cement composites", *Journal of Advanced Concrete Technology*, Vol. **1**(3), 241-252.
- Parra-Montesinos, G.J. (2005), "High-performance fiber-reinforced cement composites; an alternative for seismic design of structures", *ACI Structural Journal*, Vol. **102**(5), 668-675.
- Paulay, T. and Priestley, M.J.N. (1992), *Seismic Design of Reinforced Concrete and Masonry Buildings*, Wiley & Sons, New York, NY, 768 pp.